

Evaluation of TIGBT field stop layer generated by helium implantation

Radim Pechal^{*}, Lubomír Dorňák, Juraj Vavro, Adam Kozelský, Adam Klimsza

ON Semiconductor, 1. máje 2230, 756 61 Rožnov pod Radhoštěm, Czech Republic
^{*}e-mail: radim.pechal@onsemi.com

A helium implantation is a common technique used for electron and hole lifetime control in semiconductor devices. Siemieniec [1] shows that suitable annealing conditions after the helium implantation lead to an increased conductivity of N-type silicon substrate in the affected area. Based on these observations a possibility of using helium implantation for generation of the TIGBT field stop layer was evaluated. Required concentration profiles were prepared for test wafers, however, a decreased conductivity in the helium implantation area was observed when using production wafers with standard process flow. The root cause of this discrepancy is diffusion of nitrogen and hydrogen atoms into the silicon during previous diffusion operations and an interaction of these atoms with the implanted helium.

1. Introduction

A trench insulated gate bipolar transistor (TIGBT) is a common semiconductor device, which is typically used as an electronic switch in power applications. A structure of a new TIGBT device during its development is optimized with respect to several parameters: break down voltage, V_{ceon} , turn-off power losses, etc. Those parameters are interdependent. Power losses can be improved by drift region thickness reduction but TIGBT with thinner drift region has lower break down voltage. This decrease can be compensated by including an additional layer called field stop layer (FS). This structure has been published by Laska [2].

One way in which FS layer can be generated is implantation of phosphorus into back-side of the wafer after a wafer thinning process. The implanted layer is then activated by a furnace annealing. An active dose is limited by a maximum furnace annealing temperature, which is typically limited by the melting temperature of a metallization present on a front side of the wafer. Those limitations can be avoided by using different elements like hydrogen or helium, which has lower level of energy required for their activation in silicon matrix.

The results of field stop layer generated by multiple hydrogen implantations were published by Niedernostheide [3]. This solution is covered by a patent [4]. Results of TIGBT with FS layer generated by helium have not been published yet.

An electrical characterization of helium implantation into the silicon wafer has been studied by Siemieniec [1]. Based on a deep level transient spectroscopy three different energy levels were identified. Two levels are near the middle of a band gap ($E_C - E_T = 0.43$ eV, $E_T - E_V = 0.35$ eV) and one level is close to a conduction band ($E_C - E_T = 0.17$ eV). The concentrations of those three levels depend on the annealing conditions. The levels near to the middle of the band gap are dominant for the low temperature annealing ($\sim 300^\circ\text{C}$). An effective dopant concentration for N-type substrate decreased for these conditions. The level close to the conduction band is dominant for higher temperature annealing ($\sim 400^\circ\text{C}$ and higher) contributing to the increasing effective N-type doping concentration.

2. TIGBT field stop layer with helium implantation

A standard ON Semiconductor 1200 V FSII TIGBT [5] was used for evaluation. This TIGBT was compared to the same device with additional field stop layer generated by a helium (He) implantation. Helium was implanted with energy of 1 MeV and dose $1 \cdot 10^{13} \text{ cm}^{-2}$. The activation annealing temperature was 450°C for the duration of 30 min in nitrogen ambient. For the TIGBT with the He implantation, we expect higher break-down voltage.

The break-down voltage for TIGBT with the additional helium field stop and the standard TIGBT were similar. But the high Ice leakage (collector – emitter current) was observed (Fig. 1). A resistivity profile of TIGBT wafer measured by spreading resistance profiling technique (SRP) [6] was compared with a profile prepared on the test wafer. Both profiles are different significantly (Fig. 2).

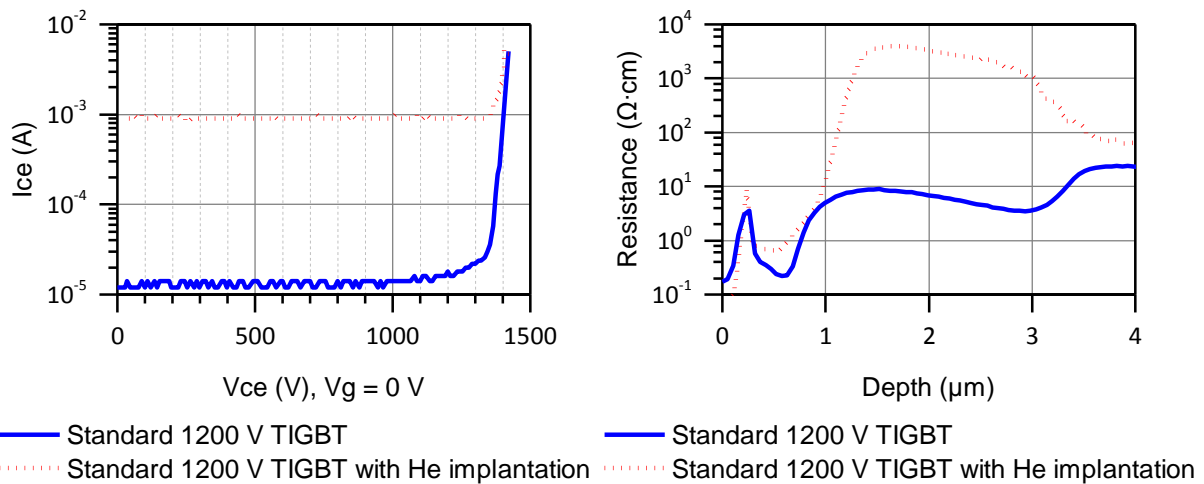


Fig. 1: Comparison of the Ice leakage for the standard 1200 V TIGBT with and without the He implantation.

Fig. 2: Back-side SRP profile of the standard 1200 V FSII TIGBT with the He implantation compared with a profile prepared on the test wafer.

3. Test wafers experiment

For the evaluation of the difference of the SRP profile between TIGBT wafer and test wafer (Fig. 2) several test wafers were prepared (summarized in table 1) and the SRP profiles were measured. In the first experiment test wafer 1 was implanted with standard phosphorus and boron (P+B) back-side implantation used for standard 1200 V TIGBT, wafer 2 was processed with the He implantation and wafer 3 was processed with a combination of the P+B back-side implantation and the He implantation. After the implantations were finished all wafers were annealed at 450°C for 30 min. The resulting resistance profiles are shown in figure 3. The resistance profile of wafer 2 decreased due to He implantation. This observation is in agreement with Siemieniecs [1]. The resistance profile for wafer 3 is a parallel combination of resistance profiles for wafer 1 and 2. This profile was expected.

Wafer 4 was processed with similar process conditions with an additional annealing between the B+P back-side implantation and the He implantation. The resistance profile in the area of He implantation did not decrease but increased (Fig. 2).

The test wafers (wafer 5, 6 and 7) without P+B back-side implantation as well as various annealing conditions preceding the He implantation were prepared to evaluate this phenomenon. The resistance profiles of those wafers are comparable with wafer 4. All wafers with the annealing before the He implantation have higher resistance in the area affected by the He implantation (Fig. 3).

Table 1: Summary of the test wafers used for the experiments and their process conditions.

Wafer	1 st step: P+B Back-side implantation	2 nd step: Annealing	3rd step: He implantation	4th step: Annealing
1	Yes	No	No	450°C 30 min
2	No	No	1 MeV 1E+13 cm ⁻²	450°C 30 min
3	Yes	No	1 MeV 1E+13 cm ⁻²	450°C 30 min
4	Yes	450°C 30 min N ₂	1 MeV 1E+13 cm ⁻²	450°C 30 min
5	No	450°C 30 min N ₂	1 MeV 1E+13 cm ⁻²	450°C 30 min
6	No	900°C 10 min H ₂ +O ₂	1 MeV 1E+13 cm ⁻²	450°C 30 min
7	No	1000°C 45 sec N ₂ +O ₂	1 MeV 1E+13 cm ⁻²	450°C 30 min

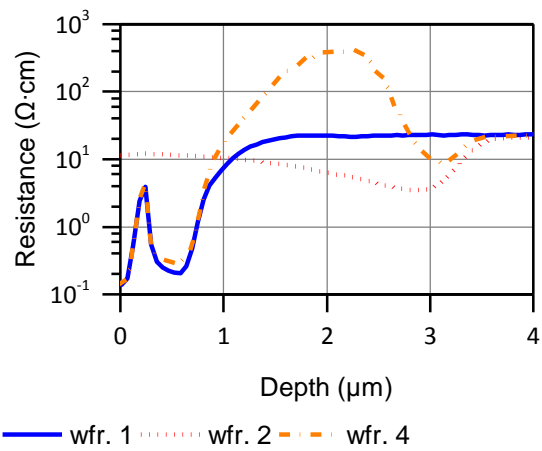
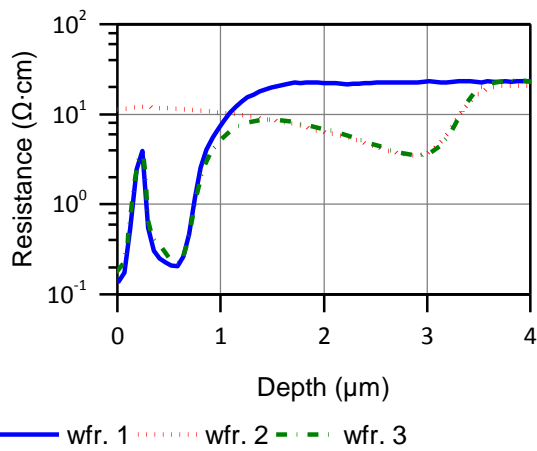


Fig. 3: Comparison of the SRP profiles of wafer 1 with the P+B back-side implantation, wafer 2 with the He implantation and wafer 3 with the combination of these implantations.

Fig. 4: Comparison of the SRP profiles of wafer 1 with the P+B back-side implantation, wafer 2 with the He implantation and wafer 4 with the combination of these implantations and the annealing before the He implantation.

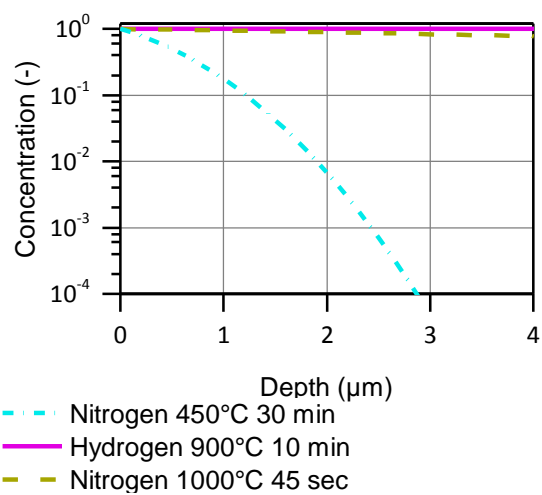
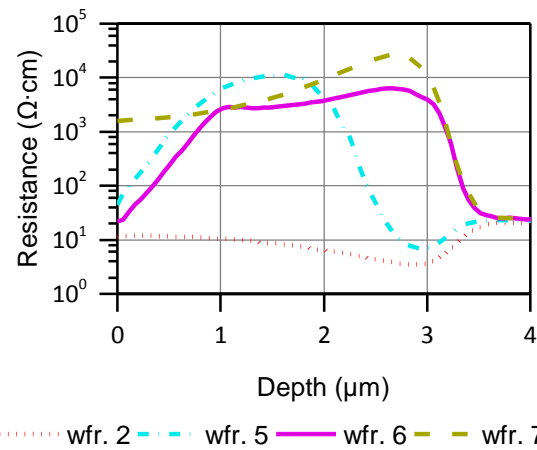


Fig. 5: Comparison of SRP profiles of wafer 2 without annealing before He implantation and the test wafers with the annealing before the He implantation.

Fig. 6: Theoretical concentration profiles of the impurities after the annealing process.

4. Interaction between the He implantation profile and the wafer process history

The He implantation resistivity profile is very sensitive to impurities or defects in the silicon. It has been demonstrated by Privitera [7], who used the He implantation as a marker for evaluation of vacancy and interstitial diffusion in silicon.

The test wafers with the annealing before the He implantation were affected by an analogous mechanism. The annealing before the He implantation was implemented in a specific furnace ambient (nitrogen, hydrogen...). Gas atoms diffused into the silicon during the process. Concentration profiles (Fig. 6) of the impurities were calculated by following formula:

$$C(\text{Depth}) \approx \operatorname{erfc}\left(\frac{\text{Depth}}{2\sqrt{Dt}}\right), \quad (1)$$

where t is an annealing time and D is a diffusion coefficient ($D_H = 6.94 \cdot 10^{-5} \text{ cm}^2 \text{ s}^{-1}$ for hydrogen at 900°C [8]). Nitrogen diffusion in silicon is a complex problem and several mechanisms have been described. If nitrogen anomalous diffusion model [9] ($D_{N 450^\circ\text{C}} = 1.51 \cdot 10^{-12} \text{ cm}^2 \text{ s}^{-1}$ for nitrogen at 450°C , $D_{N 1000^\circ\text{C}} = 2.17 \cdot 10^{-8} \text{ cm}^2 \text{ s}^{-1}$ for nitrogen at 1000°C) is used, the layer in $2 \mu\text{m}$ depth and more is affected by the hydrogen and nitrogen diffusion.

The occurrence of the impurities generated by the gas atoms diffusion into the silicon during the activation annealing is the root cause of the resistivity increase in the area affected by He implantation.

5. Conclusions

The resistance profile induced by He implantation can be significantly affected by the impurities or the defects in silicon during the He activation. Those impurities are generated by gas atoms diffusion during the annealing process preceding the He implantation.

The field stop layer generated by the He implantation is limited by the process before the He implantation. During the front-side process, a TIGBT wafer is annealed at a high temperature in an oxide atmosphere and oxygen concentration in the field stop layer reaches levels that do not allow a successful application of helium field stop layer in this process.

Acknowledgement

This work has been supported by R&D grant TH01010419 awarded by the Technology Agency of the Czech Republic.

References

- [1] R. Siemieniec et al., Compensation and doping effects in heavily helium-radiated silicon for power device applications, *Microelectronics Journal* 37.3: 204-212, 2006.
- [2] T. Laska et al., The field stop IGBT (FS IGBT)-a new power device concept with a great improvement potential, *ISPO'2000: international symposium on power semiconductor devices and IC's*, 2000.
- [3] F-J. Niedernostheide et al., Tailoring of field-stop layers in power devices by hydrogen-related donor formation, *28th International Symposium on Power Semiconductor Devices and ICs (ISPSD)*, 2016.
- [4] H-J. Schulze et al., *Semiconductor device with a field stop zone*, U.S. Patent No. 7,538,412, 2009.
- [5] ON Semiconductor, *IGBT - Field Stop II*, NGTB40N120FL2WG datasheet, Rev. 6. April, 2015.
- [6] D. K. Schroder, *Semiconductor material and device characterization*, John Wiley & Sons, 2006.
- [7] V. Privitera et al., Room-temperature migration and interaction of ion beam generated defects in crystalline silicon, *Applied Physics Letters* 68.24: 3422-3424, 1996.
- [8] *Semiconductor Technology Handbook*, Technology Associates, 1985.
- [9] V. V. Voronkov and R. J. Falster., Nitrogen diffusion and interaction with oxygen in Si, *Solid State Phenomena*, Vol. 95. Trans Tech Publications, 2004.